Nonlinear structure-composition relationships in the Ge_{1−y}Sn_{y}/Si(100) (y0.15) system

R. Beeler, R. Roucka, A. V. G. Chizmeshya, J. Kouvetakis, and J. Menéndez

Phys. Rev. B **84**, 035204 — Published 26 July 2011

DOI: 10.1103/PhysRevB.84.035204

Non-linear Structure-Composition Relationships in the $Ge_{1-y}Sn_y/Si(100)$ ($y<0.15$) system

R. Beeler,[1] *R. Roucka,*[1*] *A.V.G. Chizmeshya,*[1] *J. Kouvetakis,*[1] *and J. Menéndez*[2]

[1]Department of Chemistry and Biochemistry, Arizona State University, Tempe AZ 85287-1504

[2]Department of Physics, Arizona State University, Tempe, AZ 85287-1504

February 21, 2011

The compositional dependence of the cubic lattice parameter in $Ge_{1-y}Sn_y$ alloys has been revisited. Large 1000-atom supercell *ab initio* simulations confirm earlier theoretical predictions that indicate a positive quadratic deviation from Vegards' law, albeit with a somewhat smaller bowing coefficient, θ = 0.047 Å, than found from 64-atom cell simulations (θ = 0.063 Å). On the other hand, measurements from an extensive set of alloy samples with compositions $y < 0.15$ reveal a negative deviation from Vegard's law. The discrepancy with earlier experimental data, which supported the theoretical results, is traced back to an unexpected compositional dependence of the residual strain after growth on Si substrates. The experimental bowing parameter for the relaxed lattice constant of the alloys is found to be θ = -0.066 Å. Possible reasons for the disagreement between theory and experiment are discussed in detail.

PACS: 61.66.Dk, 61.50.Ah, 81.05.Cy

I. INTRODUCTION

Linear interpolation between the parent compounds is the simplest approach for estimating the properties of semiconductor alloys. While this scheme, in principle naïve, works surprisingly well for a variety of properties and material systems, applications that require very accurate values of certain parameters have prompted systematic studies of departures from linearity. A

good example is the compositional dependence of band gaps. In laser or detector devices, the exact emission or cut-off wavelengths are of primary importance, and therefore even small deviations from linearity may be of practical significance in this context. Similarly, a detailed knowledge of the deviations from Vegard's law[1] in the compositional dependence of the lattice constant can be used for accurate determinations of the alloy composition using X-ray diffraction.

The deviations from linear behavior in the compositional dependence of alloy properties are often characterized by introducing bowing parameters (quadratic coefficients). The magnitude of these bowing parameters has been successfully correlated with the mismatch in size and electronic properties between the constituent atoms.[2] For example, a comparative study of the optical properties of $Si_{1-x}Ge_x$ and $Ge_{1-y}Sn_y$ alloys[3] reveals much larger bowing parameters in the latter, which has been attributed to the larger difference in atomic sizes as well as electronegativities. In the case of the cubic lattice parameter, a small negative deviation from linearity was observed in $Si_{1-x}Ge_x$ alloys,[4] whereas a small positive departure was reported for $Ge_{1-y}Sn_y$ alloys.[5] This qualitatively different behavior has been confirmed in a number of *ab initio* theoretical studies.[5-9]

The different signs of the bowing parameters in $Si_{1-x}Ge_x$ and $Ge_{1-y}Sn_y$ alloys provide a unique insight into the origin of the deviations from Vegard's law. Using a simple structural model of the alloys that assumes force constants independent of the bond nature, Mousseau and Thorpe showed that in a $Si_{1-x}Ge_x$ alloy the observed negative deviation from Vegard's law obtains if the equilibrium heteronuclear Si-Ge bond length is smaller than the average of the homonuclear Si-Si and Ge-Ge lengths.[10] However, they were unable to confirm that this is the main cause of bowing, since they lacked an independent way to determine the equilibrium bond

lengths and they could not rule out other factors, such as different force constants or clustering effects. Strong evidence for the bond-length origin of the bowing was provided by Chizmeshya *et al*., who studied solid-state systems as well as molecular analogs consisting of tetrahedral clusters of the form $A(BH_3)_4$, where A and B can be C, Si, Ge, or Sn.[5] Their crucial finding is that the difference between heteronuclear and average homonuclear bonds in the molecular compounds is about the same, in magnitude and sign, as in the corresponding solid phases. In particular, the trends in the molecular compounds are in perfect agreement with the predicted positive bowing in $Ge_{1-y}Sn_y$ alloys and negative bowing in $Si_{1-x}Ge_x$ alloys.

While the work of Chizmeshya *et al*. provides a convincing framework for understanding the origin of bowing in the compositional dependence of the lattice constant in group-IV alloys, the problem cannot be considered definitively solved because the smallness of the quadratic terms make their theoretical evaluation and experimental determination quite challenging. On the theoretical side, earlier *ab initio* theoretical calculations for $Si_{1-x}Ge_x$ alloys indicated a positive deviation from linearity,[11] in disagreement with the experimental results from Dismukes *et al*.,[4] and with more recent calculations.[12,13] This suggests that convergence issues, as well as artificial correlations introduced by the small supercells used to simulate the alloy, may affect the predicted deviations from linearity. Accordingly, we have carried out *ab initio* lattice constant calculations in very large (1000 atom) supercells, which provide a statistically accurate description of the random alloy. We optimized the supercell cell shape, dimensions, and internal atomic positions to obtain highly converged equilibrium structures with residual cell stresses less than 1 kbar and atomic forces less than 5 meV/Å. These calculations confirm the earlier predictions of a positive deviation from Vegard's law.

On the experimental side, the problem is particularly difficult because bulk-like $Ge_{1-y}Sn_y$ samples are not available, and the measurements must be performed on epitaxial alloys on Si substrates. A good illustration of the experimental difficulties associated with thin film measurements is provided by the work of Kasper *et al*,[14] who determined the lattice parameter in $Si_{1-x}Ge_x$ films grown pseudomorphically on Si and could only verify Dismukes' earlier bulk data[4] in a semi-quantitative way due to the uncertainties in the Ge concentrations and in the strain corrections. In the case of $Ge_{1-y}Sn_y$ alloys, the experimental evidence so far is based on measurements of $Ge_{1-y}Sn_y$ films grown directly on (001) Si.[5] In this work, the *c* lattice constant perpendicular to the growth plane was obtained from the (004) x-ray reflection in the tetragonally distorted diamond structure. In view of the low residual strain in the samples, the measured *c* was identified with the relaxed cubic lattice constant a_0. The systematic error incurred by using this approximation does not affect the sign of the quadratic term in the compositional dependence of the lattice constant as long as the residual strain can be assumed to be the same for all samples, a reasonable assumption at the time. In subsequent years, however, we have accumulated increasing evidence that this residual strain is strongly correlated with the alloy composition, to the extent that a systematic error might be introduced in the determination of the bowing parameters for the alloy if a strain correction is not applied. In view of these complications, we have measured *x*-ray reciprocal space maps (RSMs) of the (224) reflection for a large set of $Ge_{1-y}Sn_y$ alloys grown on Si substrates. From these measurements we extract the relaxed cubic lattice parameter, and we find that the deviation from Vegard's law is negative. Thus we conclude that that there is a remaining disagreement between theory and experiment in the case of $Ge_{1-y}Sn_y$ alloys. The experimental lattice constant bowing parameter for the $Ge_{1-y}Sn_y$ alloy, however, is less than the bowing parameter for the $Si_{1-x}Ge_x$ alloy as a fraction of the lattice

constant mismatch between the parent elemental semiconductors, whereas the bowing parameters for all other measured properties are much larger in $Ge_{1-y}Sn_y$ than in $Si_{1-x}Ge_x$. This suggests that the data may be viewed as a qualitative confirmation of theory if we assume that the predicted trend to positive bowing in $Ge_{1-y}Sn_y$ alloy is overcompensated by an intrinsic or extrinsic contribution that is unaccounted for in the theoretical simulations.

The remainder of the paper is organized as follows: in Sect. II we present the new theoretical simulations, in Sect. III we present the new experimental data, and in Section IV we discuss the divergent conclusions from theory and experiments and analyze possible reasons for the discrepancy.

II. THEORY

For the alloy simulation we adopted 1000-atom super-cells comprised of a 5x5x5 array of conventional 8-atom crystallographic cells, in which the Sn and Ge atoms are randomly distributed on the available sites. We specifically consider two alloy compositions: the first containing 50% Sn, where any deviations from average behavior are expected to be close to maximal, and a 10% Sn model which overlaps with the high end of the composition range explored in our study. The latter is expected to provide a useful point of comparison with experiment. The 1000-atom super cell models represent a significant refinement over our earliest calculations for this system in which much smaller 64-atom super cells were used to describe Sn_yGe_{1-y} alloy compositions with Sn content from 0-50%.[5] In this case, however, highly symmetric ordered atomic distributions were used in order to make the calculations tractable. In subsequent work on related $Si_{1-y}Sn_y$ alloys we incorporated the random nature of the alloys using both discrete 64-atom distributions, as well as special quasi-random (SQS) cells.[15] In this regard the present treatment using the very large supercells is expected to inherently capture most

random lattice pair-correlations up to about the 6th nearest neighbor. As we shall show below, our $Ge_{1-y}Sn_y$ simulations yields nearly Gaussian bond species distributions which follow the expected limiting statistical behavior based on concentration products, namely y^2, $2y(1-y)$ and $(1-y)^2$ for Sn-Sn, Sn-Ge and Ge-Ge bonds, respectively. For a 1000-atom diamond lattice unit cell, the number of bonds is 2000 (e.g., four bonds per tetrahedral site, times ½ for double counting). Thus, for example, for 10% Sn concentration our $Ge_{1-y}Sn_y$ alloy representation should contain 20 Sn-Sn bonds, 360 Sn-Ge bonds and 1620 Ge-Ge bonds. In practice we find that our random configurations contain distributions that deviate from these ideal values by only 1-2 bonds, suggesting that our approach should be sufficient to capture the essential structural properties of real alloys.

The ground state energy calculations of the random alloys, and elemental Ge and Sn lattices were all carried out using the VASP electronic structure code.[16,17] We employed the Ceperley-Alder parameterization of the local density functional (CA-LDA)[18,19] for exchange-correlation energy, a plane wave cutoff of 350 eV and a single *k*-point centered at Γ, which is found to be adequate in view of the large lattice dimensions (~30 Å). Special precautions were taken to ensure that the calculations of the elemental α-Ge and α-Sn reference system properties and those of the alloys are performed consistently, and at the same level of fidelity. In particular, we ensured that all internal integration grids and sampling procedures were identical in all cases, and that all symmetrizations were explicitly "switched off". Using these computational conditions we then simultaneously optimized the supercell shape and dimensions, and the atomic positions, to obtain very accurate equilibrium structures with a residual cell stress and atomic forces of less than ~1 kbar and ~0.005 eV/Å, respectively.

The key outcomes of our study are summarized in Table 1 which lists the electronic ground state energies U_0 and lattice parameters a_0 for the elemental reference states (α-Ge and α-Sn), as well as the compositionally average (Vegard) values corresponding to 10% and 50% Sn content. Note that energies produced by VASP (listed here as U_0) are relative to spin-compensated neutral atoms, and not spin-polarized ground state configurations. All of the lattice constants listed in the table correspond to a conventional crystallographic cell, and were obtained by dividing the supercell edge length by 5 (small distortions in edge length ~0.001 Å were averaged). Our LDA values for the lattice constants of α-Ge and α-Sn are 0.57% and 0.49% smaller than their corresponding experimental values at room temperature. Since the calculations correspond to static values, a more meaningful comparison is with low-temperature lattice constants corrected for zero-point vibrational expansion. The experimental static values are extrapolated from the asymptotically linear temperature dependence observed at high temperatures,[20] and proceeding this way we find the that the differences between theory and experiment are reduced to 0.46% (α-Ge) and 0.35% (α-Sn). The residual discrepancy is typical for this level of DFT. Also listed in the table are values from our prior work which were obtained using a similar DFT treatment at the CA-LDA level using the much small a 64-atom setting, but a higher cutoff energy (600 eV), and a 3x3x3 Monkhorst-Pack sampling for reciprocal space integrations. The agreement is clearly very good, and the small discrepancies are entirely due to the different computational conditions used.

The bottom portion of Table 1 summarizes the key energetic and structural results for the alloys, including their equilibrium lattice constants a_0, ground state electronic energies U_0, and their corresponding deviations from compositionally weighted average (Vegard) values, Δa_0 and ΔU, respectively. We note that the arbitrary spin-compensated *atomic* reference states (discussed above), contained in the U_0 values generated by VASP, cancel in the calculation of ΔU. Accordingly, the latter represent the electronic contribution to the formation energies of an $Ge_{1-y}Sn_y$ alloy relative to its pure Sn and Ge end members. On the basis of the calculated ΔU listed here, the 10% and 50% random SnGe alloys are predicted to be metastable by ~19 and ~48 meV/atom, respectively. Also listed for comparison is the corresponding ΔU value ~29 meV/atom for the symmetric zinc-blende configuration of the $Ge_{0.5}Sn_{0.5}$ alloy, which is found here to possess a slightly lower electronic energy than the corresponding random alloy (e.g., less metastable). To more quantitatively describe the thermodynamic stability of the alloys we

	U_0 (eV/atom)	ΔU (eV/atom)	ΔG (eV/atom)	a_0 (Å)	Δa_0 (Å)
α-Sn	-4.5008 -4.5016[(a)]	--	--	6.4574 6.4557[(a)] ***6.4894***	--
α-Ge	-5.1969 -5.1980[(a)]	--	--	5.6250 5.6261[(a)] ***5.6575***	--
***x*Sn+(1-*x*)Ge (*x*=0.5)**	-4.8489	--	--	6.0412	--
***x*Sn+(1-*x*)Ge (*x*=0.1)**	-5.1273	--	--	5.7082	--
α-$Ge_{0.9}Sn_{0.1}$ (RAND)	-5.1079	+0.0194	+0.0110	5.7127	0.0045
α-$Ge_{0.5}Sn_{0.5}$ (RAND)	-4.8009	+0.0480	+0.0301	6.0529	0.0117
α-$Ge_{0.5}Sn_{0.5}$ (ZB)	-4.8197	+0.0292	+0.0292	6.0522	0.0110

Table 1: Summary of energetic and structural results for the $Ge_{1-y}Sn_y$ super cell calculations. Experimental values are shown in bold font, and those from our prior study (Ref. 5) using 64-atom cell representations for α-Ge and α-Sn are indicated by a superscript (a). The free-energy estimates ΔG are obtained by combining the molar mixing enthalpy and an ideal mixing formula for mixing entropy at T=300K.

calculated the alloy Gibbs free energy *G=H-TS*. For simplicity we ignore the vibrational contributions to the free energy (assumed to be small in comparison to ΔU) and approximate the alloy enthalpy of mixing ΔH by $\Delta U_{SnGe}^{MIX}(y) \approx \Delta E_{SnGe}(y) = E_{SnGe}(y) - yE_{Sn} - (1-y)E_{Ge}$. For the corresponding entropy contribution to the free energy we assume an ideal mixing formula, $TS_{SnGe}^{MIX}(y) = -k_B T[y \ln y + (1-y)\ln(1-y)]$, which yields 8.40 meV/atom and 17.92 meV/atom for the 10% and 50% random alloys, respectively. With these approximations the Gibbs free energy ΔG of the random and ordered systems are predicted to be nearly identical, differing by only a few meV/atom near ambient conditions, while at higher temperatures the mixing entropy is expected to favor the random alloy.

The equilibrium lattice constants a_0 of the alloys obtained from our simulation are listed in the bottom right hand portion of the table, along with their corresponding deviations from compositionally averaged (Vegard) values, Δa_0. For both compositions the deviations are predicted to be positive, and the nominal bowing parameter, assuming a dependence of the form

$$a_0(y) = a_0^{\mathrm{Ge}}(1-y) + a_0^{\mathrm{Sn}} y + \theta^{\mathrm{GeSn}} y(1-y), \qquad (1)$$

is found to be θ^{GeSn} = 0.0468 Å, quite close to the value θ^{GeSn} = 0.063 Å reported in our earlier study on $Ge_{1-y}Sn_y$[5] as well as in other studies.[6,8] We note that the bowing parameter obtained in the present study for the perfectly ordered zincblende configuration is θ^{GeSn} = 0.0440 Å, which is perhaps surprising in view of its radically different bonding topology (e.g., the presence of exclusively Sn-Ge bonds).

Equilibrium structures for the calculated alloys are shown in Figure 1, where the Sn atoms are represented by grey spheres and the tetrahedral lattice, including the Ge atoms, are drawn using faint blue lines for clarity. The supercell parameters a_{SC} and lattice constants $a=a_{SC}/5$ are listed below these figures. The parameter $\langle b_{SC} \rangle$ provided above the structure model represents an "intrinsic bond length" obtained from the macroscopic cell dimension ($\frac{\sqrt{3}}{4}a$). In the zinc-blende structure (and elemental diamond lattices) $\langle b_{SC} \rangle$ is precisely equal to the unique tetrahedral bond length in the system. The Ge-Ge, Sn-Ge and Sn-Sn bond distributions obtained from our 1000-atom simulations of the 10% and 50% Sn alloys are plotted in the right panels of **Figure 1**, and exhibit nearly Gaussian forms for

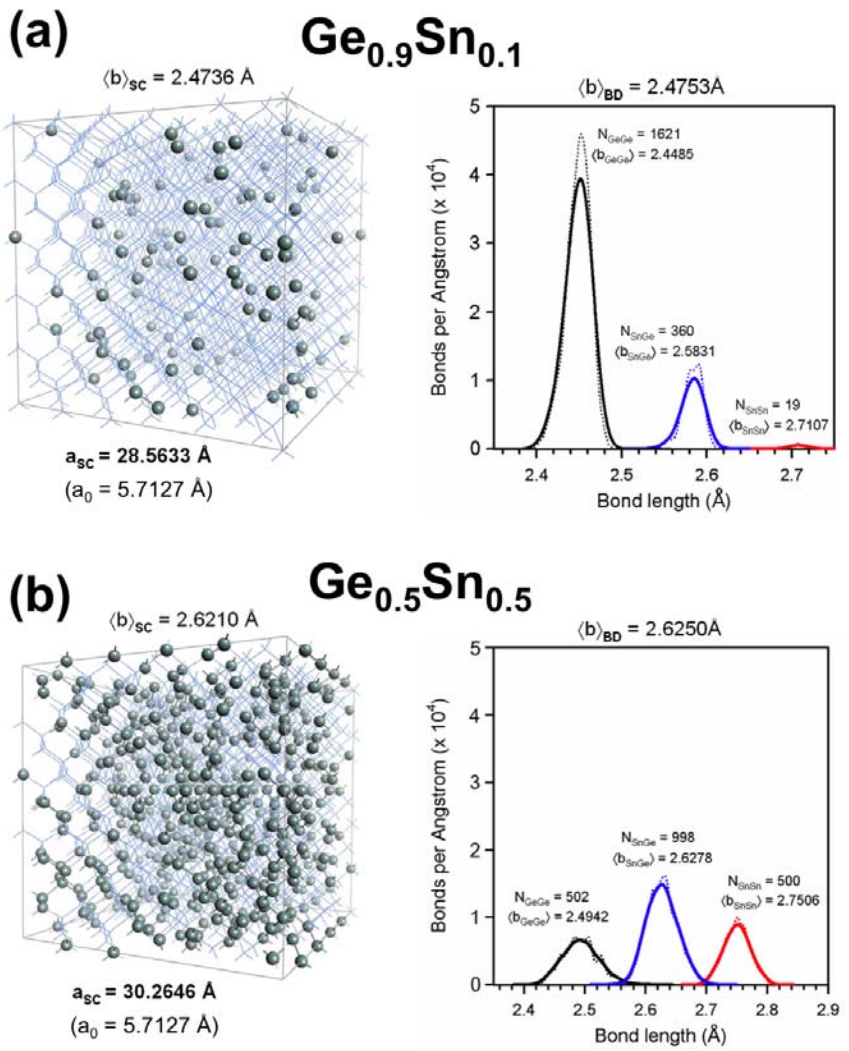

Figure 1: Bond distribution analysis of the $Sn_{0.1}Ge_{0.9}$ (a) and $Sn_{0.5}Ge_{0.5}$ (b) random alloy models. Representative structures for the alloys are shown in the left panels with the diamond lattice, including Ge positions, drawn using faint blue lines and grey spheres representing the Sn atoms. Plots on the right show the corresponding distributions for GeGe (black), SnGe (blue) and SnSn (red) bonds. The number of bonds, and mean bond lengths for each species are indicated within the figures. The values $\langle b \rangle_{BD}$ and $\langle b \rangle_{SC}$ are the average bond lengths obtained from the weighted bond distributions and macroscopic crystal dimensions, respectively.

all species. The mean bond length $\langle b_{ij} \rangle$ listed above each distribution function is calculated by dividing the first moment of the distribution by its integrated area (equal to the number of bonds, listed as *N*). Finally, above each plot we list the mean bond length $\langle b_{BD} \rangle$ obtained for each alloy from the weighted sum of individual mean bond lengths $\langle b_{ij} \rangle$. For disordered binary alloy systems such as $Ge_{1-y}Sn_y$, characterized by relatively compressible bonds, our simulations correctly embody the fundamental deviations of bonds lengths from their natural values as deduced from the elemental end members and interpolation between these latter values. Variations on the order of 2-4% are typical, as illustrated in Table 2, which lists the characteristic Ge-Ge, Sn-Ge and Sn-Sn bond lengths obtained from our simulations of elemental Ge and Sn, and the GeSn alloys.

	Ge-Ge	***Sn-Ge***	***Sn-Sn***
α-Ge	2.436	--	--
$Ge_{0.9}Sn_{0.1}$	2.449	2.583	2.711
$Ge_{0.5}Sn_{0.5}$	2.494	2.628	2.751
α-Sn	--	--	2.796

Table 2: Characteristic bond lengths in the $Ge_{1-y}Sn_y$ alloys and elemental Sn and Ge calculated using 1000-atom supercells.

III. EXPERIMENT

$Ge_{1-y}Sn_y$ films were grown on (001) Si substrates via reactions of SnD_4 with Ge_2H_6, as described elsewhere.[21] Rutherford backscattering (RBS) via the RUMP program was used to determine the Sn-concentration and film thickness,[22] which varied from about 800 nm for the lowest Sn concentrations to about 90 nm for $y = 0.13$. The calculated areal density is obtained by modeling the system as a diamond structured $Ge_{1-y}Sn_y$ alloy. This approach is found to perfectly reproduce the thickness of the layers as measured by XTEM and from ellipsometric determinations. In a typical acquisition of the random spectrum the sample is continuously rotated to avoid channeling. Typically 10^5 counts are collected at a beam energy of 0-2 MeV corresponding to 350 channels, which ensure a high signal to noise ratio sufficient for resolving

Sn contents as low as 0.1 %. This technique is ideally suited for these binary alloys because the atomic number of both constituent elements are high and sufficiently distinct to enable a clear (unambiguous) separation of their signals.

In addition to thickness and composition the degree of crystallinity and epitaxial alignment of the films is also gauged by RBS analysis using the ratio of the aligned versus random peak heights (χ_{min}). In our samples it decreases from 10% at the interface to 5 % at the surface, indicating a reduction in dislocation density across the thickness of the film. The 5 % value approaches the limit $\chi_{min} \sim 3\%$ observed in a perfect Si crystal, suggesting that most of the defects accommodating the lattice mismatch between film and substrate are confined at the interface. This is consistent with high-resolution transmission electron microscopy XTEM pictures showing essentially defect-free films. The concentration of residual threading defects and the mosaic spread of the crystal are improved by performing a few—typically three—rapid-thermal annealing (RTA) cycles of 2-30 s each at temperatures between 600 °C and 750 °C. This post-growth processing reduces the FWHM of the (004) rocking curve in high-resolution X-ray diffraction measurements (HR-XRD).

The HR-XRD measurements of the lattice constant were carried out at room temperature using a PANalytical-diffractometer. The in-plane—*a*—and perpendicular—*c*—tetragonal lattice parameters of 56 $Ge_{1-y}Sn_y$ samples and 14 reference Ge films on Si were determined from measurements of the (004) $2\theta/\omega$ peaks and reciprocal space maps (RSM) of the (224) reflection. The pure Ge films had a range of thicknesses comparable to those of the $Ge_{1-y}Sn_y$ alloys and were grown using the method described in Ref. 23. The samples were first aligned to the Si(004) reflection and the position of the $Ge_{1-y}Sn_y$ (004) peak was measured. From the $Ge_{1-y}Sn_y$ (004) peak position the *c*-lattice parameter and a possible lattice tilt was calculated. In all cases the tilt

was found negligible. After that the sample was aligned to the corresponding Si (224) reflection and the $Ge_{1-y}Sn_y$ (224) reflection was measured. The in-plane and out-of-plane lattice parameters were determined from the 224 peak maxima. For a subset of the samples we measured the four (224), $(\bar{2}24)$, $(2\bar{2}4)$, and $(\bar{2}\bar{2}4)$ reflections to confirm the tetragonal nature of the distortion and establish a limit for the inherent error of the method. All of the *c* lattice parameters determined from (224) reflections were found to match match the value obtained from the (004) reflections to within 0.0004 Å. The relaxed cubic lattice constant a_0 was computed from the measured *a* and *c* parameters using

$$a_0 = \frac{c + \frac{2C_{12}}{C_{11}} a}{1 + \frac{2C_{12}}{C_{11}}}, \tag{2}$$

where C_{11} and C_{22} are cubic elastic constants in the contracted index notation. The elastic constant ratio is taken as

$$\frac{C_{12}}{C_{11}} = 0.3738 + 0.1676y - 0.0296y^2 \tag{3}$$

The independent term in Eq. (3) is the value of C_{12}/C_{11} in pure Ge as reported by McSkimin.[24] The compositional dependence of C_{12}/C_{11} was obtained from a quadratic interpolation of the *ab initio* theoretical calculations in Ref. 25.

For the pure Ge films on Si the use of Eqs. (2) and (3) gives a_0 = 5.6571±0.0004 Å. This is in very good agreement with the value a_0 = 5.6574 Å quoted in Ref. 26 as the average of all data for pure Ge compiled from 1922 to 1968. For the samples for which the four (224) were measured, the relaxed lattice parameters a_0 were found to be nearly identical, with typical standard deviations of ~0.0001 Å. In Fig. 2 we show the a, c, and a_0 values for the $Ge_{1-y}Sn_y$ samples. The calculated value of a_0 for the alloys is in principle affected by the accuracy of the compositional dependence of the elastic constant ratio in Eq. (3), for which there is no experimental corroboration. However, we notice that the exact value of C_{12}/C_{11} is not as critical as in the $Si_{1-x}Ge_x$ experiments reported in Ref. 14, because the strain levels in our samples are about one order of magnitude lower, and therefore the uncertainties in the compositional dependence of the elastic constant ratio have a substantially reduced impact on the final a_0 value. In fact, the bowing parameter for the compositional dependence of a_0 (see below) remains virtually unchanged if we ignore the compositional dependent terms in Eq. (3) and simply use the pure Ge value from McSkimin.[24]

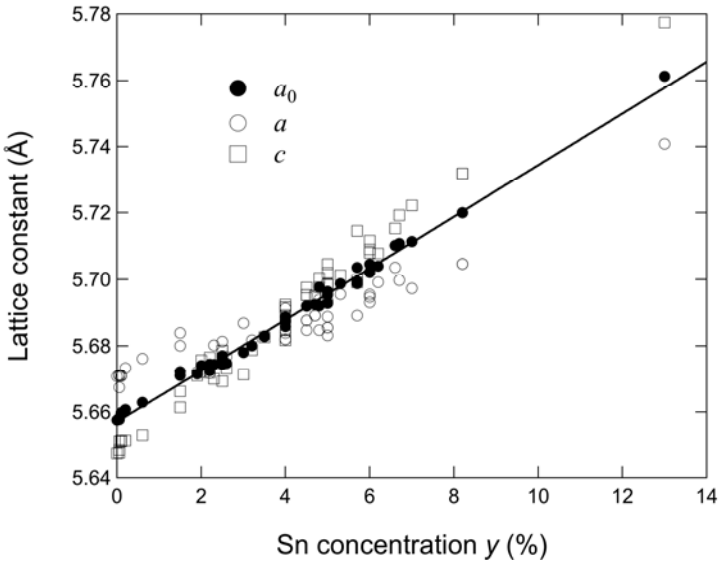

Figure 2: Experimental lattice constants a (parallel to growth plane) and c (perpendicular to the growth plane) obtained from room-temperature HR-XRD RSM measurements of $Ge_{1-y}Sn_y$ films on Si. The relaxed cubic lattice constant a_0 is calculated from these values using Eqs. (2) and (3). The solid line is a fit with Eq. (1). Notice that the residual strain is tensile ($a > c$) for low Sn-concentrations, and becomes compressive ($a < c$) for high Sn-concentrations.

It is apparent from Fig. 2 that for low Sn concentrations $a > c$, whereas for high Sn concentrations $a < c$. This indicates a gradual transformation of the nature of the in-plane strain $\varepsilon_P = (a - a_0)/a_0$ from tensile at low Sn-concentrations to compressive at the highest Sn concentrations, as shown in Fig. 3.

If the films are perfectly relaxed during growth, we would expect the residual strain at room temperature to be tensile due to the smaller thermal expansion coefficient of the Si substrate relative to the $Ge_{1-y}Sn_y$ film. This is in fact the approach used to obtain tensile-strained Ge films on Si.[27] The presence of compressive strain indicates an incomplete strain relaxation while the sample is growing. While the higher Sn concentration may by itself inhibit the generation of the required misfit dislocations, the most likely reason for the incomplete strain relaxation is the lower growth temperatures used to deposit films with high Sn concentrations. These lower temperatures also reduce the growth rate, which leads to a monotonic decrease in film thickness as a function of the Sn concentration. Thus we cannot rule out the possibility that the degree of strain relaxation during growth depends not only on the growth temperature but also on film thickness. Interestingly, our post-growth annealings increase the tensile strain only marginally, as seen in Fig. 3, even though the annealing temperatures are much higher than the film growth temperatures. At even higher annealing temperatures one expects the samples to relax and

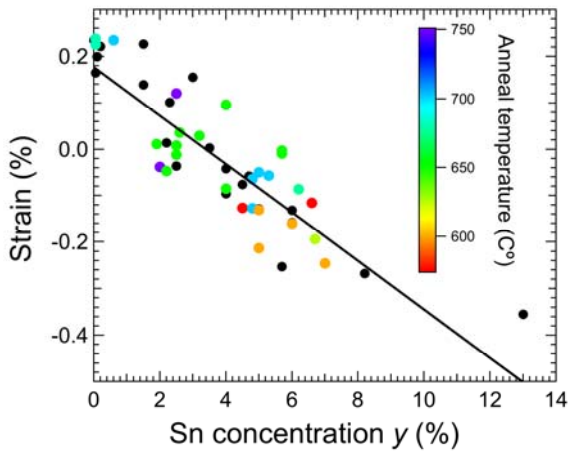

Figure 3: In-plain strain $\varepsilon_P = (a - a_0)/a_0$ computed from the data in Fig. 2 for all $Ge_{1-y}Sn_y$ samples. The color code indicates the after-growth rapid thermal anneal (RTA) temperatures for the different samples. Black circles correspond to samples measured as-grown without any RTA treatment. The line is a linear fit to the strain.

develop tensile strain upon cooling to room temperature, regardless of the growth temperature. The threshold annealing temperature for this behavior seems to be close to 725 °C for pure Ge films, but this limit is difficult to explore in $Ge_{1-y}Sn_y$ alloys because the Sn concentration may change at the highest temperature annealings.

The simplest way to show that the data in Fig. 2 deviate from Vegard's law is to fit the a_0 values to a linear function of composition. This fits gives $a_0(0)$ = 5.6571±0.0004 Å, in perfect agreement with the directly measured Ge lattice constant, but $a_0(1)$ = 6.428±0.010 Å for α-Sn, which is substantially *below* the experimental value a_0 = 6.4894 Å at 300K.[28] This clearly indicates a negative deviation from Vegard's law. The disagreement with the earlier finding of a positive deviation can be traced back to the fact that the measured *c*-parameter increases faster than a_0 as a function of Sn-concentration, as seen in Fig. 2, due to the monotonic change in the residual strain from tensile to compressive. The solid line in Fig. 2 shows a fit with Eq. (1). Since the compositional range of the data is limited, a fit that uses a_0^{Ge}, a_0^{Sn}, and θ^{GeSn} as adjustable parameters gives a negative value for θ^{GeSn}, as expected, but an unphysical value for a_0^{Sn}. We thus perform the fit using a_0^{Sn} = 6.4894 Å as a fixed parameter, and in order to treat both end values on equal footing we also use a fixed a_0^{Ge} = 5.6571 Å. We are then left with θ^{GeSn} as the only adjustable parameter, and we obtain θ^{GeSn}

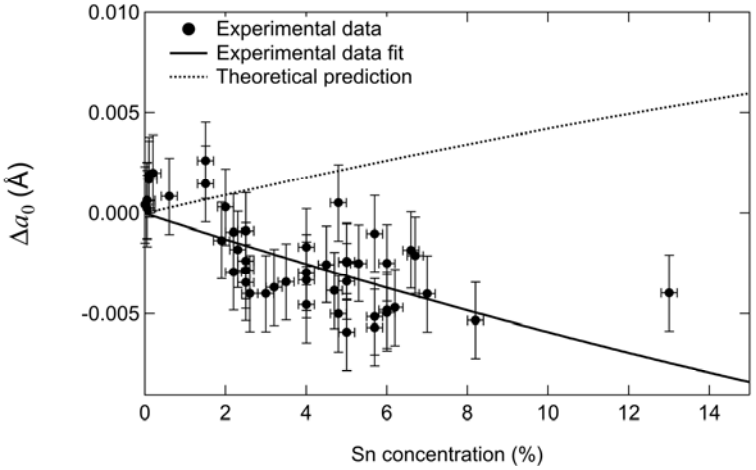

***Figure 4**:* Deviation Δa_0 from Vegard's law for the lattice constant of $Ge_{1-y}Sn_y$ alloys. The lines correspond to the function $\theta^{GeSn}\, y(1-y)$. In the case of the solid line, we use θ = -0.066 Å from our a_0 fit in Fig. 2. The dotted line corresponds to the theoretical value θ^{GeSn} = +0.0468 Å. The error bars assume an error of ±0.2% in the composition determined by RBS.

= -0.066±0.005 Å. We have verified that the value of θ^{GeSn} remains virtually unchanged if we use any of the published values for the lattice constant of α-Sn (similarly, if we use a_0^{Ge} as an adjustable parameter we obtain a_0^{Ge}= 5.6573±0.0004 Å and θ^{GeSn} = -0.069±0.009 Å). The deviation from Vegard's law $\Delta a_0 = a_0(y) - a_0^{Ge}(1-y) - a_0^{Sn}y$ is shown in full detail in Fig. 4.

IV. DISCUSSION

The significance of the discrepancy between the theoretical predictions and the new measurements for $Ge_{1-y}Sn_y$ is difficult to assess. If we assume that the experimental compositional dependence of the deviation from Vegard's law is quadratic (hardly obvious from our data given the noise and the limited compositional range), the difference between predicted and actual lattice constant for $Ge_{0.5}Sn_{0.5}$ would be 0.46%, which is comparable to the error in the best DFT-LDA predictions of lattice constants. On the other hand, DFT-LDA calculations seem to correctly predict bowing in other semiconductor alloy systems, so the discrepancy in the case of $Ge_{1-y}Sn_y$ seems puzzling. Moreover, we note that the predicted lattice constant error for α-Sn is less than that for Ge. If we assume a correction factor that depends linearly on the alloy composition, this would add an additional small but *positive* contribution to the bowing, increasing the discrepancy with theory. The agreement is better at the lowest Sn concentrations ($y < 0.02$), as seen in Figure 4. This could be fortuitous, given the limited number of data points and large error bars, but we have already found that at these same low Sn concentrations the bowing parameter for the direct electronic gap E_0 appears to be significantly larger than the value obtained from samples with $y > 0.02$.[29,30] These observations, taken together, suggest that some structural change might take place near $y \sim 0.02$. S-shaped deviations from Vegard's law have been explained in terms of the contribution from bond-bending forces.[31] For sufficiently large values of these forces, the bonds are prevented from expanding or compressing following atomic

substitutions. However, since such effects are automatically included in *ab initio* calculations, we should have observed some anomaly in the theoretical compositional dependence of both lengths if the deviation from Vegard's law has an oscillating behavior as a function of the Sn concentration. A convenient way to study bond lengths in terms of the competition between bond-bending and bond-stretching forces is provided by the so-called topological rigidity parameter a^{**} (Ref. 32). This parameter measures of the difference between interatomic bond lengths and the macroscopic lattice constant – a very relevant and useful figure of merit for the comparison of structural properties within a compositional family of alloys. A value of $a^{**}= 0$ corresponds to the completely rigid lattice (Vegard limit) in which bond-bending forces dominate and bonds lengths take on equal values to match the macroscopic lattice parameter. The opposite $a^{**}=1$ case represents the so-called Pauling limit in which bond stretching forces are dominant, so that all bond length species take on their natural values and bond angle deviations accommodate the competition between macroscopic dimensions and the local bond-lengths. For a $Ge_{1-y}Sn_y$ alloy the a^{**} can be deduced by fitting the bond distributions for various compositions y in a random alloy to the formulas:

$$\begin{aligned} \langle L_{GeGe} \rangle &= \bar{L} - ya^{**}(L^0_{SnSn} - L^0_{GeGe}) \\ \langle L_{SnSn} \rangle &= \langle L_{GeGe} \rangle + a^{**}(L^0_{SnSn} - L^0_{GeGe}) \\ \langle L_{SnGe} \rangle &= \tfrac{1}{2}\left[\langle L_{GeGe} \rangle + \langle L_{SnSn} \rangle\right] \end{aligned} \qquad (4)$$

where the quantities in $\langle ... \rangle$ brackets represent average bond length values in the alloy, the L^0 are the natural (unique) bond lengths obtained from the pure phases, and the average bond length is defined $\bar{L} = yL^0_{SnSn} + (1-y)L^0_{GeGe}$. Using the data provided in Figure 1 and Table 2, our 1000-atom simulations yields $a^{**}=0.685$ for $Ge_{0.9}Sn_{0.1}$ and $a^{**}=0.693$ for $Ge_{0.5}Sn_{0.5}$. These values are remarkably consistent in view of the significant difference in Sn content between the two alloys,

and very similar to the corresponding the average value of a^{**}~0.68 obtained in our prior studies on 12 GeSn alloy compositions between 0-50% Sn, using 64-atom supercells. It is noteworthy that Shen *et al*.[6] also reported a value of a^{**}~0.69 for the $Ge_{1-y}Sn_y$ alloy on the basis of three compositions (y = 0.25, 0.50 and 0.75) using a 72-atom supercell setting. Collectively, the forgoing evidence suggests a universal value of a^{**}=0.69 for $Ge_{1-y}Sn_y$ based on DFT-LDA. Thus the ratio of bond-bending to bond-stretching forces seems to be independent of the composition, which is incompatible with an oscillating dependence of the deviation from Vegard's law near the low-Sn compositional range. Recently we also carried out a comparative topological rigidity analysis of the bonding in $Si_{1-y}Sn_y$ alloys[15] (also using 64-atom supercells) and obtained a value of a^{**}~0.72. Direct experimental measurements of a^{**} are extremely difficult and only available for the $Si_{1-x}Ge_x$ alloy, where values of a^{**} in the range of 0.6-0.8 have been reported in the literature.[11,33-35]

Yet another interpretation of the discrepancy between theory and experiment would consist in assuming that the observed deviation from Vegard's law is caused by the combined effects of a positive contribution, as calculated for a perfectly random alloy, plus a negative term associated with a non-random atomic distribution and/or defects. This is suggested by the observation that the ratio $\eta^{GeSn} = \theta^{GeSn} \Big/ \left(a_0^{Sn} - a_0^{Ge}\right)$, which measures the size of the non-linear deviation relative to the lattice mismatch between the parent materials, is η^{GeSn} = 0.089, whereas the equivalent quantity for $Si_{1-x}Ge_x$ alloys is η^{SiGe} = 0.12. Since we find $\eta^{SiGe} < \eta^{GeSn}$ for the electronic properties,[3] the observation that $\eta^{SiGe} > \eta^{GeSn}$ for the lattice constant could be viewed as a qualitative confirmation of the theoretical predictions under an scenario in which the trend towards a positive bowing is overcompensated by the second effect.

A good measure of the importance of randomness in the predicted alloy lattice constants is provided by a comparison of a_0 calculated for the random $Ge_{0.5}Sn_{0.5}$ alloy and for the ordered zincblende GeSn compound. The finding that these lattice constants are nearly identical suggests that ordering effects do not play a dominant role in this system. On the other hand, we notice that the so-called Sn-split vacancies, in which Sn atoms are located at the bond-center site between two missing Ge atoms,[36] lead to a decrease in lattice parameter. For example, Ventura and coworkers find a cubic lattice parameter of 5.77Å for pure Ge, 5.82 Å for a $Ge_{15}Sn_1$ alloy, and 5.72 Å for a $Ge_{14}Sn_1$ alloy with a split vacancy.[37] The abundance of these defects is related to the vacancy concentration,[38] which may not be constant as a function of Sn concentration due to the different growth temperatures. Based on the Ventura *et al.* results,[37] we estimate that about 6% of the Sn atoms in the alloy should be in split vacancy locations to explain the difference between the observed and predicted lattice parameter for $y = 0.06$. This is a much higher concentration of split vacancies than predicted by these authors, and constitutes a level of non-substitutionality that likely would have been detected in our XRD or RBS channeling experiments.

V. CONCLUSIONS

In summary, we have revisited the compositional dependence of the lattice constant in $Ge_{1-y}Sn_y$ alloys from a theoretical and experimental perspective. While the theoretical calculations confirm the positive deviation from Vegard's law predicted by earlier work, the experimental results indicate a clear negative deviation, in contradiction with earlier data which were affected by the residual strain in $Ge_{1-y}Sn_y$ films grown on Si. Different scenarios have been analyzed to explain the discrepancy, but no fully satisfactory explanation can be provided at this time.

VI. ACKNOWLEDGEMENTS

This work was supported by the U.S. Air Force under contract DOD AFOSR FA9550-06-01-0442 (MURI program), by the Department of Energy under contract DE-FG36-08GO18003, and by the National Science Foundation under grant DMR-0907600.

REFERENCES

*Radek.Roucka@asu.edu

1 L. Vegard, Zeitschrift für Physik **5**, 17 (1921).
2 J. E. Bernard and A. Zunger, Phys. Rev. B **36** (6), 3199 (1987).
3 V. R. D'Costa, C. S. Cook, A. G. Birdwell, C. L. Littler, M. Canonico, S. Zollner, J. Kouvetakis, and J. Menendez, Phys. Rev. B **73** (12), 125207 (2006).
4 J. P. Dismukes, L. Ekstrom, and R. J. Paff, J. Phys. Chem. **68** (10), 3021 (1964).
5 A. V. G. Chizmeshya, M. R. Bauer, and J. Kouvetakis, Chemistry of Materials **15** (13), 2511 (2003).
6 J. Shen, J. Zi, X. Xie, and P. Jiang, Phys. Rev. B **56** (19), 12084 (1997).
7 Y. Chibane, B. Bouhafs, and M. Ferhat, phys. stat. sol. (b) **240** (1), 116 (2003).
8 A. Chroneos, C. Jiang, R. W. Grimes, U. Schwingenschlögl, and H. Bracht, Appl. Phys. Lett. **94**, 252104 (2009).
9 Y. Chibane and M. Ferhat, J. Appl. Phys. **107**, 053512 (2010).
10 N. Mousseau and M. F. Thorpe, Phys. Rev. B **46** (24), 15887 (1992).
11 S. d. Gironcoli, P. Giannozzi, and S. Baroni, Phys. Rev. Lett. **66** (16), 2116 (1991).
12 P. Venezuela, G. Dalpian, A. da Silva, and A. Fazzio, Phys. Rev. B **64** (19) (2001).
13 A. Chroneos, H. Bracht, C. Jiang, B. Uberuaga, and R. Grimes, Phys. Rev. B **78** (19) (2008).
14 E. Kasper, A. Schuh, G. Bauer, B. Holländer, and H. Kibbel, J. Cryst. Growth **157**, 68 (1995).
15 J. Tolle, A. V. G. Chizmeshya, Y. Y. Fang, J. Kouvetakis, V. R. D'Costa, C. W. Hu, J. Menéndez, and I. S. T. Tsong, Appl. Phys. Lett. **89** (23), 231924 (2006).
16 G. Kresse and J. Furthmüller, Phys. Rev. B **54** (16), 11169 (1996).
17 G. Kresse and J. Hafner, J. Phys: Condens. Matter **6** (40), 8245 (1994).
18 D. M. Ceperley and B. J. Alder, Phys. Rev. Lett. **45** (7), 566 (1980).
19 J. P. Perdew and A. Zunger, Phys. Rev. B **23** (10), 5048 (1981).
20 M. Cardona, Solid State Commun. **133** (1), 3 (2005).
21 M. Bauer, J. Taraci, J. Tolle, A. V. G. Chizmeshya, S.Zollner, D. J. Smith, J. Menendez, C. Hu, and J. Kouvetakis, Appl. Phys. Lett. **81**, 2992 (2002).
22 L. R. Doolittle, Nuclear Instruments and Methods in Physics Research Section B: Beam Interactions with Materials and Atoms **9** (3), 344 (1985).

[23] M. A. Wistey, Y. Y. Fang, J. Tolle, A. V. G. Chizmeshya, and J. Kouvetakis, Appl. Phys. Lett. **90** (8), 082108 (2007).
[24] H. J. McSkimin, J. Appl. Phys. **24** (8), 988 (1953).
[25] J. Kouvetakis, J. Menendez, and A. V. G. Chizmeshya, Annual Review of Materials Research **36**, 497 (2006).
[26] O. Madelung, in *Landolt Börstein* (Springer-Verlag,, Berlin, New York, 2001), Vol. 41-Aα.
[27] D. D. Cannon, J. Liu, Y. Ishikawa, K. Wada, D. T. Danielson, S. Jongthammanurak, J. Michel, and L. C. Kimerling, Appl. Phys. Lett. **84** (6), 906 (2004).
[28] J. Thewlis and A. R. Davey, Nature **174** (4439) (1954).
[29] V. R. D'Costa, Y. Fang, J. Mathews, R. Roucka, J. Tolle, J. Menendez, and J. Kouvetakis, Semicond. Sci. Technol. **24** (11), 115006 (2009).
[30] J. Mathews, R. T. Beeler, J. Tolle, C. Xu, R. Roucka, J. Kouvetakis, and J. Menéndez, Appl. Phys. Lett. **97** (22), 221912 (2010).
[31] C. Y. Fong, W. Weber, and J. C. Phillips, Phys. Rev. B **14** (12), 5387 (1976).
[32] Y. Cai and M. F. Thorpe, Phys. Rev. B **46** (24), 15872 (1992).
[33] J. C. Woicik, C. E. Bouldin, M. I. Bell, J. O. Cross, D. J. Tweet, T. M. Zhang, L. B. Sorensen, C. A. King, J. L. Hoyt, P. Pianetta, and J. F. Gibbons, Phys. Rev. B **43** (3), 2419 (1991).
[34] D. B. Aldrich, R. J. Nemanich, and D. E. Sayers, Phys. Rev. B **50** (20), 15026 (1994).
[35] J. C. Aubry, T. Tyliszczak, A. P. Hitchcock, J. M. Baribeau, and T. E. Jackman, Phys. Rev. B **59** (20), 12872 (1999).
[36] S. Decoster, S. Cottenier, U. Wahl, J. G. Correia, and A. Vantomme, Phys. Rev. B **81** (15) (2010).
[37] C. Ventura, J. Fuhr, and R. Barrio, Phys. Rev. B **79** (15) (2009).
[38] A. Chroneos, H. Bracht, R. W. Grimes, and B. P. Uberuaga, Appl. Phys. Lett. **92** (17), 172103 (2008).